2019-24-0184

Inner-Insulated Turbocharger Technology to Reduce Emissions and Fuel Consumption from Modern Engines

Author, co-author (Do NOT enter this information. It will be pulled from participant tab in MyTechZone)

Affiliation (Do NOT enter this information. It will be pulled from participant tab in MyTechZone)

Abstract

Reducing emissions from light duty vehicles is critical to meet current and future air quality targets. With more focus on real world emissions from light-duty vehicles, the interactions between engine and exhaust gas aftertreatment are critical. For modern engines, most emissions are generated during the warm-up phase following a cold start. For Diesel engines this is exaggerated due to colder exhaust temperatures and larger aftertreatment systems. The De-NOx aftertreatment can be particularly problematic. Engine manufacturers are required to take measures to address these temperature issues which often result in higher fuel consumption (retarding combustion, increasing engine load or reducing the Diesel air-fuel ratio).

In this paper we consider an inner-insulated turbocharger as an alternative, passive technology which aims to reduce the exhaust heat losses between the engine and the aftertreatment. Firstly, the concept and design of the inner-insulated turbocharger is presented. A transient 3D CFD/FEM (Computation Fluid Dynamics/ Finite Element Modelling) simulation is conducted and predicts that external heat losses will be reduced by 70% compared to a standard turbocharger, i.e. non-insulated turbocharger. A 1D modelling methodology is then presented for capturing the behaviour of the inner-insulated turbocharger. This is important as conventional models based on isentropic efficiency maps cannot accurately predict turbine outlet temperature. The alternative model is essential to demonstrate benefits in system-level simulations. Experimental results are presented from a transient air-path testing facility to validate the 1D model and demonstrate the characteristics of the inner-insulated turbocharger. Finally, the validated 1D model is used within a powertrain optimization simulation to demonstrate an improvement in fuel consumption for iso-NOx emissions over a low load city cycle of up to 3%.

The work was conducted under the THOMSON project which has received funding from the European Union's Horizon 2020 Program for research, technological development and demonstration under Agreement no. 724037. The project aims to increase the market penetration of 48V hybrid vehicles.

Introduction

Hybridization using 48V systems is a technology that will enable the fast market penetration of hybrid-electric light duty vehicles because of its relatively low cost. However, introducing this level of electrical power opens up the possibility of many new technologies that can have significant impact on emissions and efficiency of the powertrain. These include large starter motors that are capable of launching the vehicle, the use of electrically assisted boosting systems, electric thermal management systems and electrically heated catalysts. The increase in electrical load also offers a prime route for collecting and using electrical energy recuperated via regenerative braking.

The new 48V systems will increase the complexity of energy flows within the powertrain and these need to be carefully managed and optimized in order to maximize the performance of the complete system. This remains true for all new technologies which could interact with the electrical system, one of which is the focus of this paper.

Future internal combustion engines will be more efficient which leads to significantly lower exhaust gas temperatures. The limits of the next exhaust gas legislation standards applied on real driving emission (RDE) driving cycles will result in load cycles with arbitrary engine speeds, engine load conditions that will lead to arbitrary temperature distributions inside engine components along the gas paths. The engine exhaust gas aftertreatment systems (EAT) requires new approaches to guarantee a high efficient pollutions (NOx, HC, CO) conversion within these load cycles [1, 2]. Therefore mechanism are recommend to ensure faster EAT activation.

Current engines incorporate methods to promote rapid light-off of the EAT [3-5] but these include an engine efficiency penalty. For example, retarding combustion reduces engine thermal efficiency but increases exhaust gas temperature. The air fuel ratio can be reduced by throttling the intake air, but this results in increased pumping losses. Finally additional fuel can be burnt such as during diesel particulate filter (DPF) regenerations. Whilst these approaches are effective at increasing exhaust gas temperatures at EAT inlet (commonly referred to as T4), they are clearly undesirable compromises and other approaches than engine measure are desirable. The reduction of heat losses in the exhaust paths upfront the EAT, including the exhaust manifold [6] and also the turbocharger, will keep the exhaust energy in the system for a faster activation. Another measure could involve an electrically heated catalyst to faster activate the EAT.

In this paper a turbocharger with an inner-insulated turbine housing technology is applied to a virtual 48V hybrid Diesel powertrain with a Belt Starter Generator (BSG). The EAT comprises an electrically heated catalyst (EHC), Diesel Oxygen Catalyst (DOC), a particulate filter with a coating enabling a selective catalytic reaction

(SCRF) and an underfloor catalyst for a second selective catalytic reaction (SCRuf). The inner-insulated turbocharger with a variable turbine technology is proposed to minimize heat losses between the engine cylinder and the catalysts. The inclusion of such a technology in a 48V hybrid with electrically heated catalyst is interesting because a new optimal use of the electrical component is necessary. The retention of heat in the exhaust can now be directly related to a reduction in the amount of electrical energy required to deliver the catalyst light-off.

This paper is organized as follows: the next section will present a review of research in this field. Then, the inner-insulated turbocharger concept is introduced. The following section outlines the experimental and modelling methodology. The results section then includes the major findings from the experimental and simulation results before presenting the outputs from the optimization work. The paper ends with a conclusions section.

Literature Review

Concepts for enhancing T4 on the exhaust side

This section describes different ways to enhance the exhaust temperature T4 entering the aftertreatment system by passive measures on the exhaust side. Numerous concepts have been proposed to increase T4. These can be summarized as:

- Relocation of the catalyst upstream of the turbine. This approach ensures maximum exhaust temperature flowing through the aftertreatment and also has some pumping loss benefits [5] but needs to be accompanied by a redesign of the boosting system to avoid excessive turbo-lag.
- Relocation of the catalyst in the turbine bypass, thus meaning the exhaust gases flowing to the aftertreatment have not been expanded through the turbine.
- Introduction of a turbine bypass to allow part of the exhaust flow to arrive at the aftertreatment without flowing through the turbine. This can be achieved by an active bypass valve or through a divided exhaust manifold that captures the high power part of the exhaust pulse for the turbine and the low power for heating the aftertreatment [7].
- Minimizing heat losses between the exhaust ports and the aftertreatment through insulation of the exhaust manifold and / or through the insulation the turbocharger turbine housing [6, 8, 9].

This research work fits into the last of these categories by proposing a turbocharger concept with inner-insulated turbine housing. This is by far the simplest of the approaches above as it does not require any active control and can be implemented with minimal change to the system design. Insulating the exhaust manifold has been already subject to of previous investigations and can be considered as state-of-the art technology [8].

Difficulties to modelling of T4

One-dimensional simulation is a very common method to evaluate the engine performance and perform the selection or matching of an appropriate boosting system. In these simulations, the turbine and compressor are usually modelled as maps which define the flow and isentropic efficiency characteristics. These maps are usually measured on hot gas test facility under steady conditions. The isentropic efficiencies are commonly calculated based on temperature and pressure measurements. In particular for the turbine, the actual work is calculated by the temperature rise of the gases in the compressor because of difficulties in measuring the turbine outlet temperature. Progress is being made with some advanced measurement techniques being presented to provide a direct measurement of turbine outlet temperature [10-12], but these are not yet commonplace in turbocharger characterisation. These techniques are also difficult to replicate in-situ on engine applications where space and access is usually limited.

As a consequence, the turbine maps neglect heat transfer [13, 14]. The omission of heat transfer has been shown to have negligible impacts on the engine performance prediction, especially at high loads. However, these models are not capable of accurate predictions of turbine outlet temperature (T4) [15].

In simulation, it is critical to model the heat transfer of turbocharger if turbine outlet temperature is to be correctly predicted. Three-dimensional simulation can help generate detailed flow properties of all the individual components and interfaces, based on the specific boundary conditions from experiment [16]. This will lead to the increasing of cost and time as computation fluid dynamics (CFD) simulation for thermal effects are usually complicated, and of limited practical benefit in a full system simulation. 1D simulation is cheaper and faster, though it cannot give as much details as the 3D method, but with the appropriate modelling methodology, temperatures and heat fluxes between different components can also be predicted. Lumped capacitance modelling is the widely used [17-21] in this area. It assumes the turbocharger work and heat transfer happen independently, and that the heat transfer will be divided into before and after the compression and expansion processes. The typical error in turbine outlet temperature achieved by this type of model is around 10°C [22]. However, the parameterization of these lumped capacitance models is not trivial and requires significant time as well as destructive testing to achieve the best results [23]. However, any technology that seeks to reduce heat losses in the turbocharger will require such a heat transfer model to estimate the potential system benefits.

Inner-insulated turbine housing design

The present study is focused onto the concept that deals with the minimization of the turbocharger hot end heat losses. Figure 1a reveals the assembly of an inner-insulated turbine housing (T/H) design concept, consisting of a modified T/H and insert parts (turbine inlet, volute and outlet) for enabling the insulation, to be mounted inside the T/H. The insert parts itself consist of the outer and the inner shell made out of sheet metal and a silicate insulation material in between. The outer shell is supported by bosses (highlighted with red; figure 1b) which limit relative movement between the T/H and the insulation parts [8]. The thermo-mechanical contact has been carried out by finite element analysis (FEA) analysis and highlights the support locations of the bosses where only conductive heat transfer can occur. No heat transfer is taking place at the other insulated shell surfaces. Figure 1c reveals the positioning of the outer shell during operation.

There is only a small increase in the package requirements for a T/H with an inner-insulation. Whereas the interfaces can be kept at the same position the outer T/H volute diameter slightly increases depending on the specific application. As this study covers a research project no statement about serial add-on costs can be made at this time.

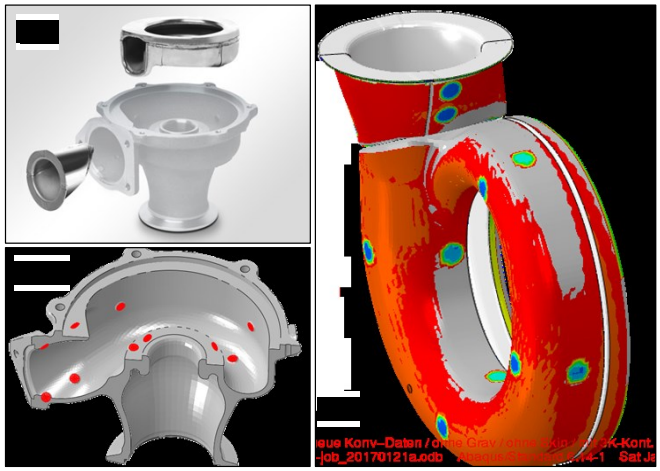

Figure 1: Inner-insulated T/H, exploded view of T/H assembly (a), T/H with structural mounting points of the inner-insulation (b) and inner-insulation with location of mounting points with T/H (c).

Methodology

The overall objective of this work is to quantify the benefits of the inner-insulated turbocharger within a 48V Diesel powertrain incorporating an electrically heated catalyst system. The system benefits will be quantified through an optimization exercise based on a systems-level simulation of the powertrain. This is achieved by comparing the performance of powertrain using the standard turbocharger compared to the inner- insulated prototype.

To capture the performance of the inner-insulated turbocharger, a 1D lumped capacitance model of the turbocharger is created which simulates the reduced heat losses compared to a conventional turbocharger. Initially a set of experiments are used to confirm that the insulation does not impact on the aerodynamic performance of the turbocharger. Then a combination of 3D simulation and experimental work is used to parameterize a 1D lumped capacitance.

Simulation approach

3D modelling approach

The best accuracy of current 3D computer aided engineering (CAE) methods will be gained by using the conjugate heat transfer (CHT) approach where momentum and energy equation of the flow field and the solid structure is coupled bi-directionally and solved simultaneously. Unfortunately, a high computational effort is required with the CHT analysis, especially in a transient solution regime. Therefore a method with a uni-directional coupling of the energy equation is used. The major benefit of this method is the usage of existing simulation models carried out for standard CAE tasks, e.g. like CFD performance analysis of the hot end flow path, conducting adiabatic thermal boundary condition and thermomechanical fatigue analysis of T/H designs. Those CAE tasks are typically conducted anyway throughout the usual product development programs. Only minor adjustments at the existing CAE models are necessary to enable them computing full transient energy balances of an entire turbocharger. In particular, an adiabatic CFD analysis is used to obtain heat transfer coefficient (HTC) and film temperatures at suitable operating conditions representing the transient thermal load cycle. These HTC boundary conditions are mapped onto the available FEA model used for standard thermal fatigue analysis. After that the adjusted FEA model is used to conduct the energy balance based onto a particular defined transient thermal load cycle.

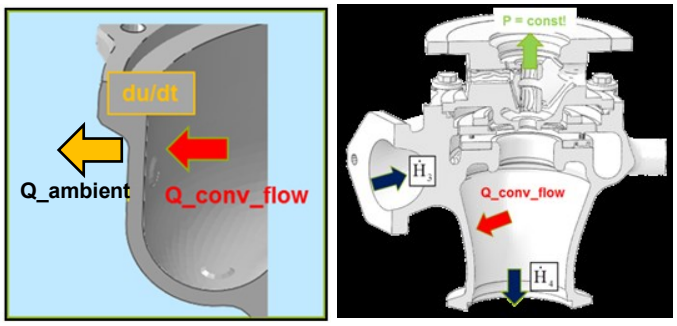

Figure 2: Heat balance approach

Figure 2 reveals the assumptions used for the CAE models. The heat loss of the flow is in equilibrium with the energy stored in the housing structure together with the heat flow to ambient. The uni-directional coupling used here neglects the temperature decrease of the flow due to the heat loss along its flow path and their impact onto the mechanical power of the turbine. Thus the heat loss of the system will be slightly higher predicted than in reality. Nevertheless the accumulated heat loss represents the T4 temperature reduction compared to the adiabatic predicted T4 temperatures what is determined by adiabatic CFD simulations. The T4 enhancement potential of the inner-insulated T/H design is carried out relatively by comparing its heat loss to the heat loss of the reference T/H what is expressed in figure 3. The difference in heat loss is a direct measure of the T4 enhancement carried out for this particular 3D computer aided design (CAD) design concept.

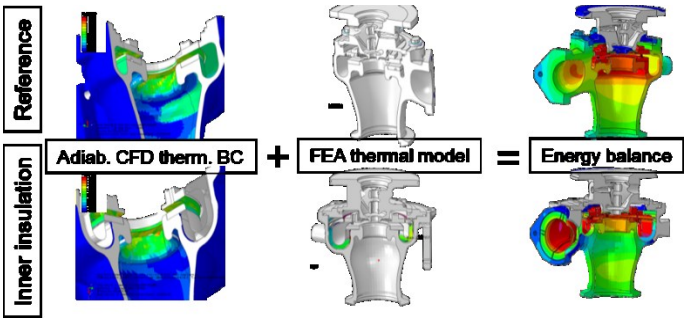

Figure 3: Approach to calculate energy balance

1D modelling approach

A simplified heat transfer model was used based on similar approaches found in the literature[13, 18, 21, 24-26] (figure 4). The model combines two thermal nodes (compressor and turbine housing), linked via conduction through the bearing housing. Heat transfer between the gases and housings can occur both before and after the compression/expansion processes which is important because of the different temperature gradients between gas and wall [27].

The focus of this section remains on the heat transfer between the exhaust gases and the turbine node. The model was implemented in MATLAB Simulink and linked to the engine modelling environment

Ricardo WAVE. The model has been parameterized based on the analysis of CAD geometry of the turbocharger and the selection of a convective heat transfer coefficient for a similar variable nozzle turbocharger system [27]. In Ricardo WAVE, two pipe templates are added pre and post the turbine, in order to take the heat transfer into account. Heat transfer fluxes are considered individually before and after turbine. It was assumed that all the heat come from gas to the wall is by convection, the Nusselt number calculation is following equation (1), in which a=0.038, b=0.662 due to the calibration [28].

$$Nu = aRe^{b}Pr^{1/3}\left(\frac{\mu_{bulk}}{\mu_{skin}}\right)^{0.14} \quad (1)$$

For radiation process:

$$Q = \sigma\varepsilon A(T_1^4 - T_2^4) \quad (2)$$

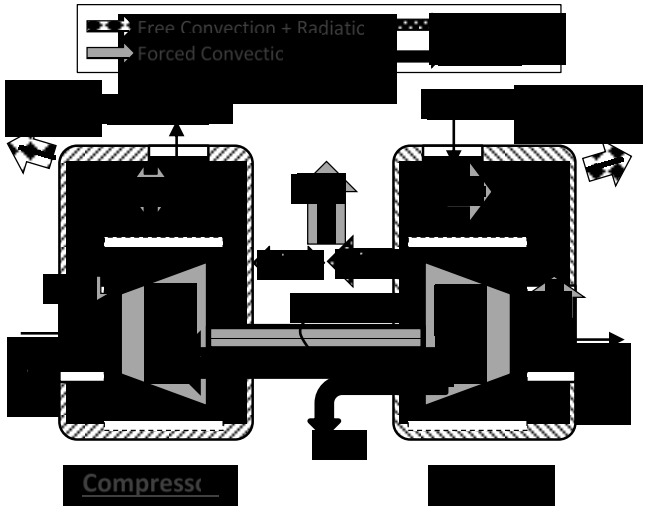

(a)

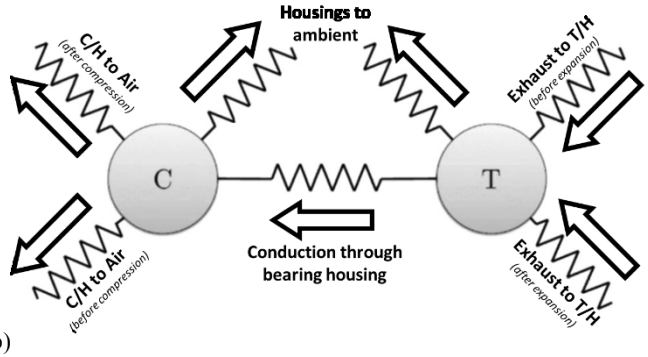

(b)

Figure 4: Overview of turbocharger heat transfer model showing (a) the conceptual layout and (b) the lumped capacitance thermal network representation.

The turbocharger heat transfer model must also include heat loss to ambient, which it has been regarded as a free convection from turbine housing to the ambient. For insulated turbine, in 1D simulation environment, the insulation will reduce the heat loss from fluid to the ambient, however, using 1D modelling to describe behaviour in the air gap between the housing and the insulation becomes difficult with many factors that are difficult to parameterize. Therefore a simpler approach is taken where an insulation factor is added into the convection process to account for the reduced heat loss from the exhaust gasses to the turbine housing. This is effectively modelled as a modification of the heat flux between the exhaust gases and the ambient by reducing the convective heat transfer from the exhaust gases to the turbine housing.

Experimental setup

Steady flow gas stand

The performance of an exhaust gas turbocharger is described hereinafter: On the compressor side by the mass flow $\dot{m}$ the compressor delivers, the corresponding pressure ratio π_{comp} (total to total pressure) and the isentropic compressor efficiency $\eta_{is\,C}$, and on the turbine side by the expansion ratio π_{exp} (total to static pressure), the turbine flow parameter TFP and the isentropic turbine efficiency $\eta_{is\,T}$. In addition there is the mechanical efficiency η_m to be considered. These values are usually plotted in maps to compare and assess different turbocharger technologies.

A special hot gas stands is applied to measure the performance of an exhaust gas turbocharger. A typical schematic overview of such a hot gas stand is shown in figure 5 where the required variables to determine the turbocharger performance (e.g. p, T) are recorded.

The turbine (T) is supplied with a hot gas mass flow at a constant temperature. The hot gas is generated in a separate device (e.g. burner) that is feed with compressed air and - quite commonly - with natural gas. The compressor (C) sucks in ambient air freely via an inlet pipe from the environment. A throttle downstream of the compressor allows to control the compressor power (not shown here).

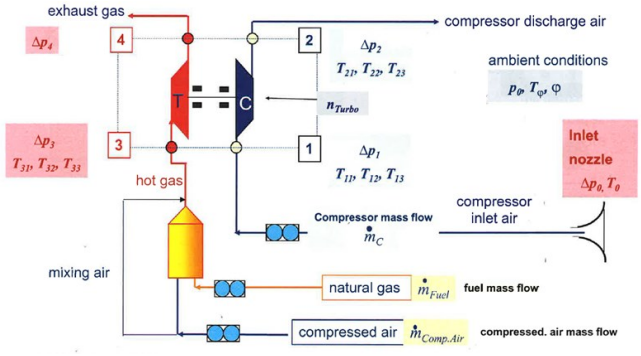

Figure 5: Schematic of a turbocharger gas stand

For constant compressor wheel tip speeds characteristic curves between the compressor surge limit and the system curve can be recorded. In this case when recording a compressor map the turbine "serves as an engine". A direct determination of the isentropic compressor efficiency $\eta_{is\,C}$ is possible because temperatures T_1, T_2 and π_{comp} can be precisely measured:

$$\eta_{is\,C} = \frac{T_{1*}\left(\pi_{comp}^{\frac{\kappa_{Air}-1}{\kappa_{Air}}} - 1\right)}{T_2 - T_1} \quad (3)$$

For plotting the compressor maps the mass flow is normalised to standard intake temperatures and pressures.

When recording turbine maps the set-up is identical. But here the compressor "serves as an engine brake". Curves with constant turbine wheel tip speeds can be recorded for constant positions of the turbine inlet guide vanes (VTG positions). In contrast to the compressor only an indirect calculation of the combined isentropic turbine and mechanical efficiency η_T is possible.

The reason for this is that it is fairly difficult to measure precisely the turbine outlet temperature T_4 to calculate the isentropic turbine efficiency $\eta_{is\,T}$ in a similar way to equation 3. In [29] new measurement techniques are introduced but these have not yet been fully established as state-of-the art techniques. Hence a different method is applied here.

As it is the fundamental principle of a turbocharger there is a balance between compressor and turbine power (equation 4).

$$\dot{m}_T * c_{p\,Exh} * T_{3t} * \left[1 - \left(\pi_{exp}\right)^{\frac{\kappa_{exh}-1}{\kappa_{exh}}}\right] * \eta_{is\,T} * \eta_{m\,T} = \dot{m}_C * c_{p\,Air} * T_{1t} * \left[\left(\pi_{comp}\right)^{\frac{\kappa_{Air}-1}{\kappa_{Air}}} - 1\right] * \frac{1}{\eta_C} * \frac{1}{\eta_{m\,C}} \quad (4)$$

Combining the mechanical efficiencies to η_m in equation 4 the overall combined turbine efficiency η_T can be derived:

$$\eta_T = \eta_{is\,T} * \eta_m \quad (5)$$

For the turbine maps the turbine mass flow is normalised to the turbine inlet temperature $T_3$and inlet pressure p_3, where as $\dot{m}_{Tred}$ can be characterised as the turbine flow parameter TFP:

$$\dot{m}_{Tred} = \dot{m}_T * \frac{\sqrt{T_3}}{p_3} \quad (6)$$

To achieve the most accurate determination of measurement variables (p,T) turbocharger gas pipes before and after the compressor and the turbine should be straight. For the sensor positions there should be enough distance to calm the flow. Pipes should be insulated to reduce heat losses for not changing the measured temperatures.

Unfortunately, in many cases all this is not possible due to application influences and test related issues and may have effects on the accuracy of the produced results. Turbine and compressor efficiencies are also influenced by many parameters, such as the wheel sizes and characteristics, wheel combination, layout of the volutes, inlet and exhaust piping, clearances, the installation situation and many others, too. Both of the wheel sizes affect π_{comp} and π_{exp}.

All in all only a certain tolerance and repeatability i.e. confidence interval can be guaranteed from hot gas stand measurements

Transient turbocharger test stand

A transient air path test facility was used to conduct transient tests in the turbochargers. A schematic of the test facility with the turbocharger is shown in figure 6. The facility can be split into three principal parts namely: a boost rig, a 2.2L diesel engine, and a gas stand-like measurement setup. The 3 principal parts are shown as dotted lines together with the instrumentation in figure 6. Individual aspects of the rig can be adjusted in all the 3 parts of the rig to achieve the required boundary conditions and turbocharger operating points. A detailed description of the test rig and its full capabilities are mentioned in [30]. The details of the sensors used and the accuracy are mentioned in Table 1.

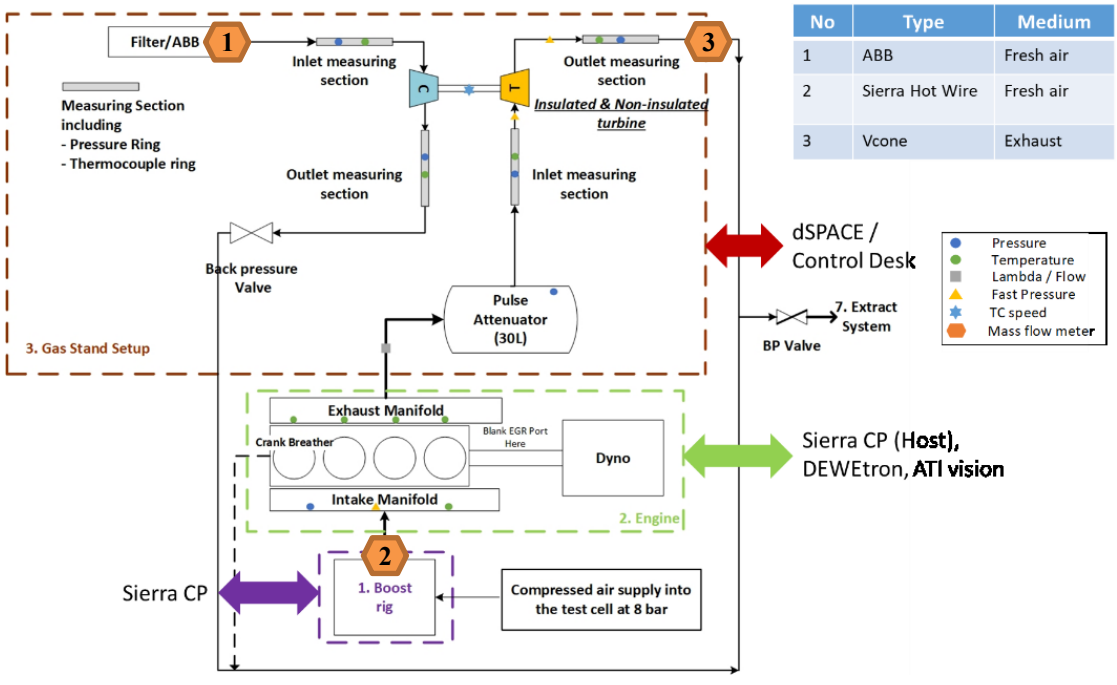

No	Type	Medium
1	ABB	Fresh air
2	Sierra Hot Wire	Fresh air
3	Vcone	Exhaust

Figure 6 Schematic of the engine gas stand setup test facility

Measurement	Sensor type and Manufacturer/Model	Accuracy / Resolution	Logging frequency
TC speed	Eddy current – Micron Epsilon DZ135 sensor	FSO resolution of ±0.22%	40Hz
Engine outlet and Turbine outlet static pressure	Water cooled Piezo-Resistive – Kistler sensors 4049B10DS1 and 4049A5s respectively	± 0.08% linearity of full scale output	10kHz
Compressor inlet and outlet static pressure	Piezo resistive silicon elementPXM419-3.5BAV and PXM419-002BGV	±0.08% FSO	40Hz
Compressor inlet air mass flow rate	ABB Sensyflow FMT700-P (hot-film anemometer)	< ± 1 % of measured value	40Hz
Average turbine/compressor/EDC inlet and outlet temperature	K Type thermocouples - TC Direct Pt100 (Precision)	± (0.15+0.002*t)	40Hz

Table 1: Sensor location, type, make, accuracy and measurement frequency of sensors in transient test stand.

Compressed air at required pressure and temperature is provided by the boost rig instantaneously. The engine utilizes the air to produce pulsating hot exhaust gas flow which is steadied using a 30L pulse attenuator before feeding it at the turbine inlet. A back pressure valve on the compressor side controls the load on the compressor which eventually determines the turbine operating point. The current experiment focuses only on the heat transfer characteristics of an inner-insulated and standard turbochargers and how it affects T4. For this purpose, similar boundary conditions are maintained and same VGT positions are used in both turbochargers.

Optimization methodology

In order to capture the total system-benefit of the inner-insulated turbocharger, a co-simulation model of all subsystems is used. This consists of 6 different, interdependent sub models. The architecture of the co-simulation models, and the interdependencies is indicated in figure 7.

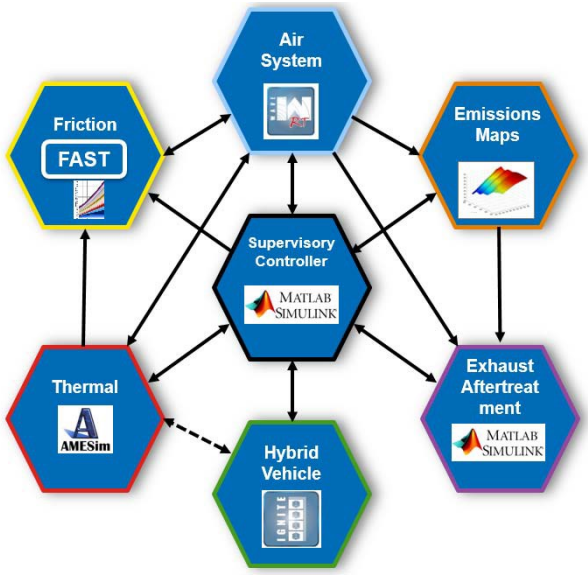

Figure 7: Co-simulation model layout for system optimization (The arrows indicate the direction of information transfer between the sub-models).

The co-simulation includes the following sub-simulations:

- Air-path and combustion (Ricardo WAVE RT)
- Engine thermal characteristics (AMESim)
- Engine frictional losses
- Emissions formation
- Aftertreatment system
- Hybrid vehicle (Ricardo Ignite)

The turbocharger models are included within the engine air-path and are integrated into the Ricardo WAVE RT simulation through co-simulation with Matlab-SIMULINK. The turbocharger heat transfer model was implemented both for the standard turbocharger and for the inner-insulated design, thus meaning the only difference between the two results is the parameterization of the heat transfer model as described earlier in this paper.

The thermal model takes the turbine inlet temperature from the WAVE-RT engine model, and uses it to calculate the heat flux and the resulting turbine outlet temperature. The calculated turbine outlet temperature is then passed to the aftertreatment models to ensure the change in temperature is captured in the predicted tailpipe emissions.

The optimization problem is set up as a constrained multi-objective optimization with two objectives: the total fuel consumption and total NOx emissions over both WLTC and NEDC duty cycles. The constraints are a requirement to meet the target brake speed and torque setpoints of the duty cycle and to respect electrical, pressure, temperature and mechanical limits of the engine components. The decision variables are the electrical power draw of the heated catalyst, the power draw of the BISG component and the total engine fuelling. These decision variables are varied at each timestep of the duty cycle. In total, four optimizations were performed: once for the NEDC and once for the WLTC for each of the standard and insulated turbochargers.

For the optimization work considered in this study, the engine calibration (in terms of EGR, AFR) will be assumed to be fixed, and hence engine out emissions maps will be used to feed the species data into the aftertreatment models. The co-simulation model will be optimized over the Worldwide Harmonized Light Vehicles Test Cycle (WLTC).

Results and Discussion

Steady flow gas stand performance

Experimental results from the steady flow gas stand tests are presented for the inner-insulated and standard turbochargers in the following section. They confirm the objectives of the inner-insulation turbine housing design which is to have no impact on the aerodynamic performance of the turbocharger. This is shown in figure 8 by the identical turbine flow characteristics (equation (6)) over the turbine

expansion ratio for the same VGT positions. The numbers in the diagrams indicate the circumferential speed in m/s for the turbine wheel for a maximally opened VTG and are the same for the other curves below in the diagram.

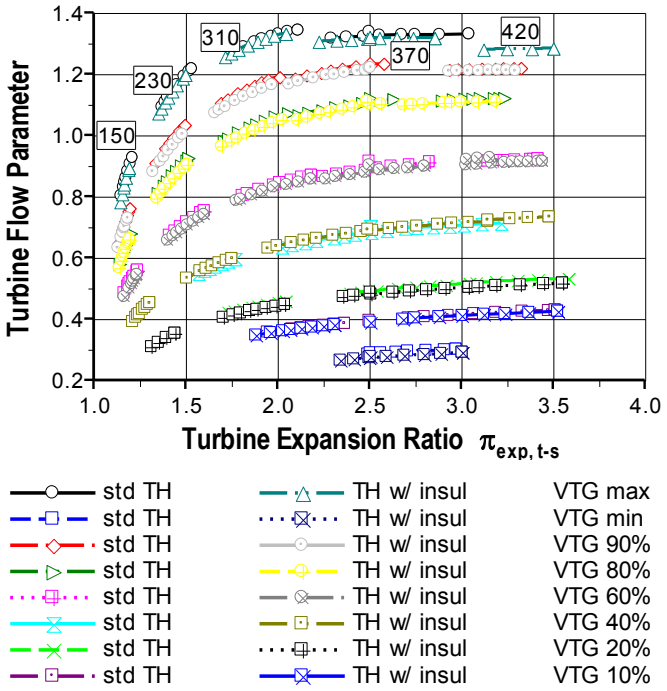

Figure 8: Turbine flow capacity map for two turbochargers with standard and inner-insulated turbine housing

Figure 9 shows the calculated turbine efficiencies (equation (5)) for both turbochargers, again compared for the same speeds and VTG positions.

For lower speeds such as 210 m/s figure 9 shows values for the isentropic turbine efficiency too high due to an over-estimation of the compressor power based on heat fluxes [29, 31]. When analysing these results more in detail for VTG position where the vanes are opened 40%, there is a small improvement in the combined turbine efficiency of ~ 2% for the inner-insulation visible (figure 10):

As mentioned before the turbine efficiency is the combined value for isentropic and mechanical efficiency. Since for this measurement a different bearing housing was applied (two different turbocharger samples) the difference could be explained by mechanical differences between both turbocharger compared here. On the other hand the inner-insulated turbine housing has a surface with different roughness values that may have influenced the isentropic efficiency. The measurements would need to be repeated again with additional samples to prove this benefit and confirm that this benefit lays not within the confidence interval for hot gas stand measurements. For the purposes of this study we confirm that there is negligible difference in aerodynamic performance between the two turbochargers.

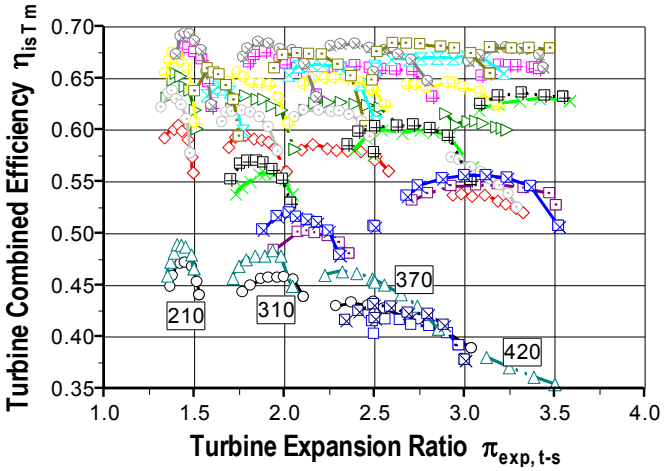

Figure 9 Efficiency map comparing two turbochargers with standard and inner-insulated turbine housing

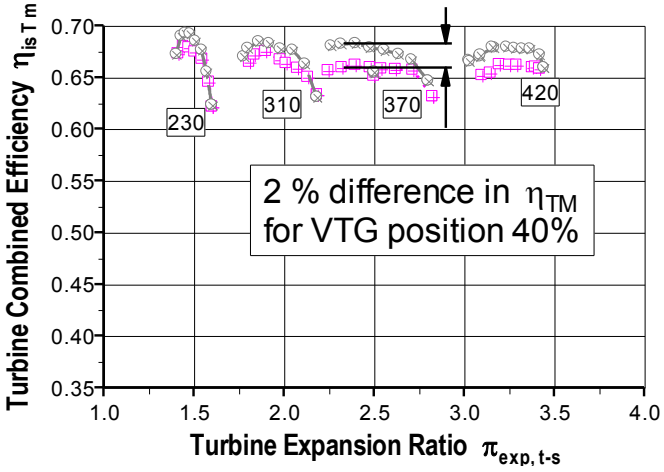

Figure 10 Efficiencies for 40% VTG position

For the comparison of the compressor maps for the turbocharger with the standard turbine housing and the turbocharger with the inner-insulated turbine housing both maps are rather comparable. There is no effect of any different heat flow into compressor housing noticeable regarding the achieved pressure ratios for the same turbocharger speeds plotted in krpm (figure 11). Nevertheless, there are some deviations: The standard turbocharger shows a gap on the left side of the map where the surge line is. But this may be explained by a different approach applied in each automated test run to detect the surge line. For high speeds, e.g. 193 krpm and above, the standard turbochargers shows slightly higher pressure ratios. This may be explained by small deviations in clearances for both turbochargers.

Regarding the isentropic compressor efficiency both turbochargers are exactly on the same level with differences below 3% for single operating points (figure 12).

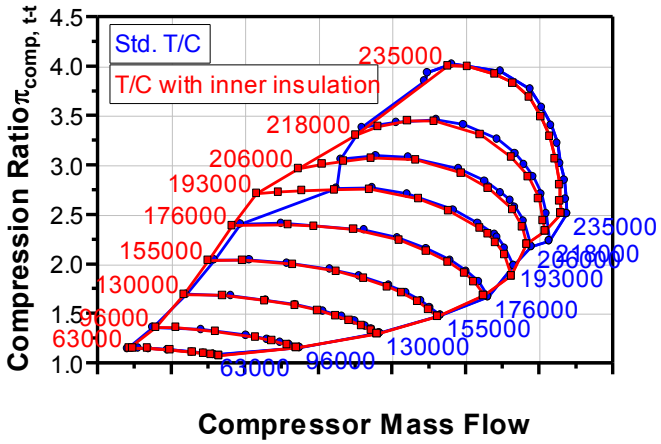

Figure 11: Compressor map comparison for the standard turbocharger and the turbocharger with inner-insulated turbine housing

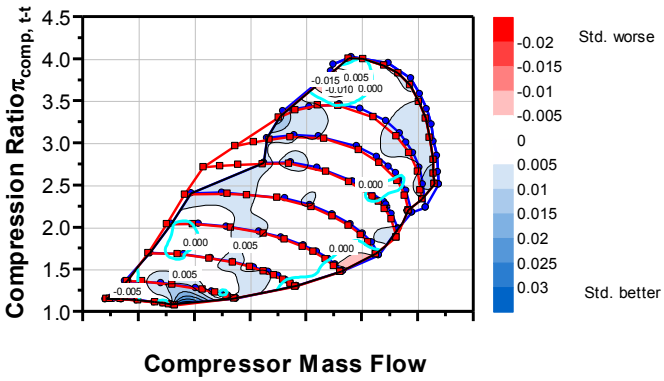

Figure 12: Comparison of isentropic compressor efficiency for the standard turbocharger and the turbocharger with inner-insulated turbine housing

3D simulation results

The 3D simulation was used to simulate a thermal-shock cycle for standard T/H fatigue analysis – shown in figure 13.

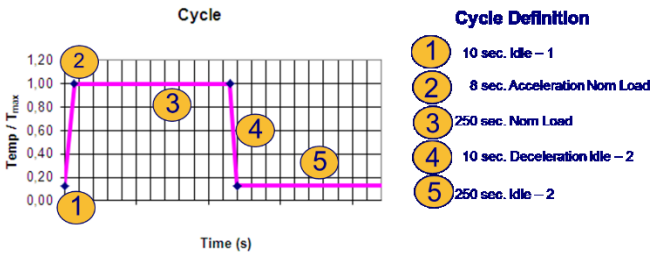

Figure 13: Defined transient load cycle

Figure 14 reveals the simulated heat fluxes of the hot gas into the volutes over this duty cycle. The inner-insulated turbocharger has reduced heat flux by 50-70% compared to the standard turbocharger. Figure 15 shows the heat fluxes to the ambient which is only 30% with the inner-insulated turbocharger.

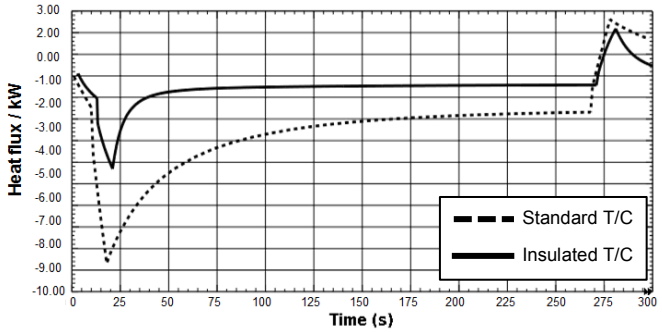

Figure 14 Heat fluxes into volute over cycle

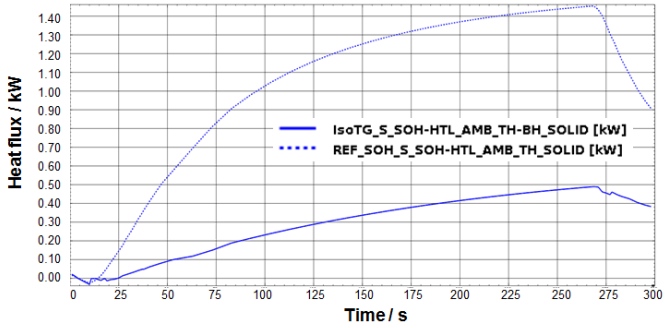

Figure 15 Heat flux to ambient

1D Model Validation

This part is captured by three steps:

1. Step-load heat transfer response from peak torque point to peak power operating point, based on the CFD thermal analysis results.
2. Turbine outlet temperature verification with experiment data, for engine cold start case.
3. Turbine outlet temperature verification with experiment data, for WLTC cycle running.

The step load simulation shown in figure 13 has been repeated in the 1D simulation to again compare the predicted heat fluxes for both turbochargers. The results from the 1D model is shown in figure 16 which has good correlation with the 3D results. As there is no engine template in the heat transfer (HT) model, the gas inlet temperature and pressure (which should be engine outlet temperature and pressure) is set to be a step profile.

A cold start experiment has been conducted on the air path test rig; alteration of the turbine inlet and outlet temperatures is used for verifying the turbine heat transfer model. K type thermocouples were used in temperature measurement which has an accuracy of ±(0.15+0.002*T). As mentioned in the literature the temperature measurement could have errors due to conduction and radiation [32] and hence T4 measurement is susceptible to errors. The ambient temperature is 300K, and the test is equivalent to holding an engine a fixed low speed/low load condition from cold. It produced the exhaust conditions of 1.25bar turbine inlet pressure 400K turbine inlet temperature once stabilized.

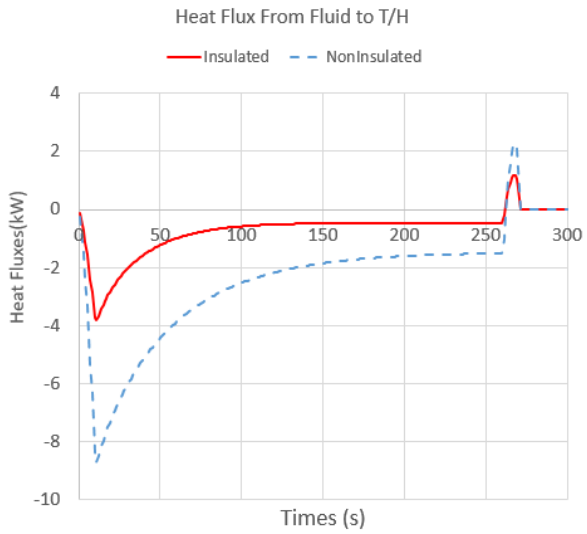

Figure 16: Comparison of the 1D models of standard and inner-insulated turbocharger for turbine heat fluxes from fluid to T/H.

The turbine outlet temperature of both experiment and simulation results are shown in figure 17. The total transient speed and trend is similar and based on this result, it can be used for predicting the thermal performance of turbine.

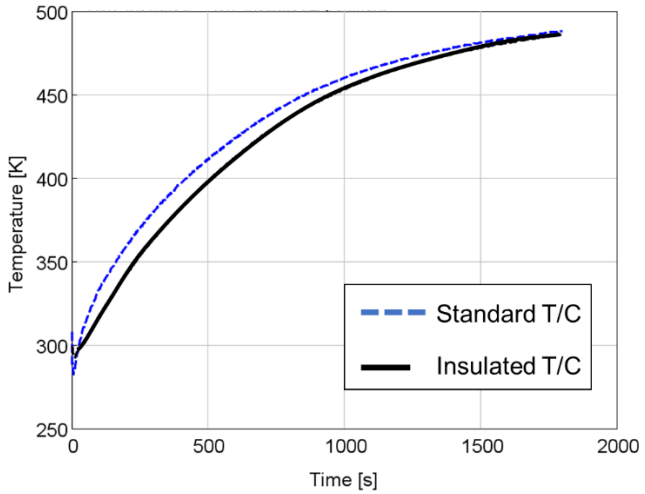

Figure 17: Turbine outlet temperature from cold start comparing simulation and experiment for the standard turbocharger and comparing simulation results for standard and inner-insulated turbocharger.

It is also interesting to investigate the inner-insulated turbocharger's benefit in an emulated WLTC cycle. figure 18a shows T4 temperature for the two turbochargers under the same inlet boundary conditions, comparing with the WLTC experiment data with the same inner-insulated turbocharger. It can be found that, for most of the time, the inner-insulated turbocharger has a higher T4 temperature than the normal one, the results is in Table 2. figure 18b shows how inner-insulated turbocharger help decreasing the heat loss from fluid to ambient.

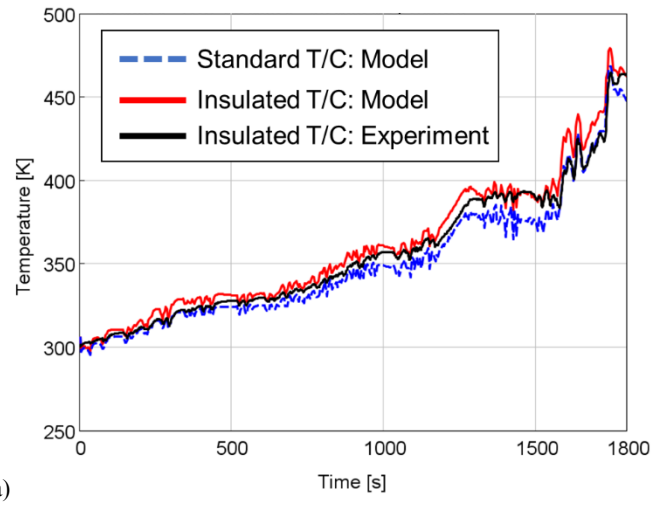

(a)

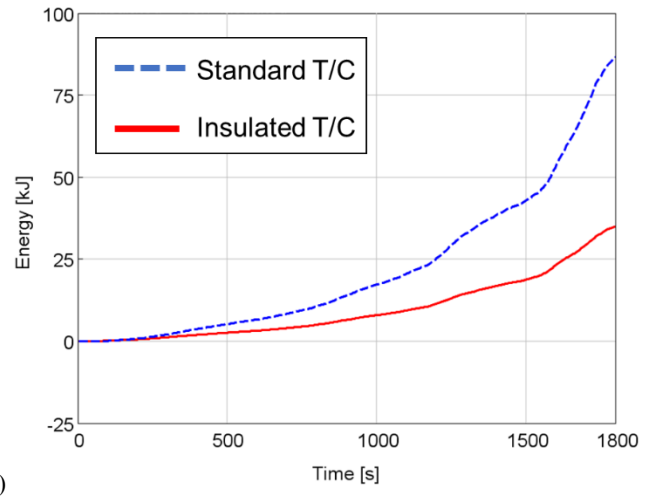

(b)

Figure 18 : (a) Turbine outlet temperature of WLTC cycle and (b) Cumulative energy loss from fluid to T/H in WLTC cycle.

		Standard	Insulated
Average T4(K)	**Simulation**	350.4	360.5
	Experiment	352.1	355.3
Simulated Energy lost (kJ)		86.8	35.1

Table 2: WLTC cycle T4 temperature and energy loss differences

Table 2 shows the post turbine temperature differences between standard and inner-insulated turbocharger in WLTC, for both simulation and experiment. In simulation, the average T4 temperature has been increased by 10.1K for insulated case. These results are overestimated compared with the experimental results. The heat loss in the turbine has also been reduced by 59.6%, which is 51.7 kJ in WLTC cycle.

Optimization Results

Results output from the optimization

For the Diesel powertrain being optimized, the initial simulation results showed an increase in turbine outlet temperature of 10 – 30 °C over the majority of the cycle – as shown over the new European driving cycle (NEDC) in figure 19.

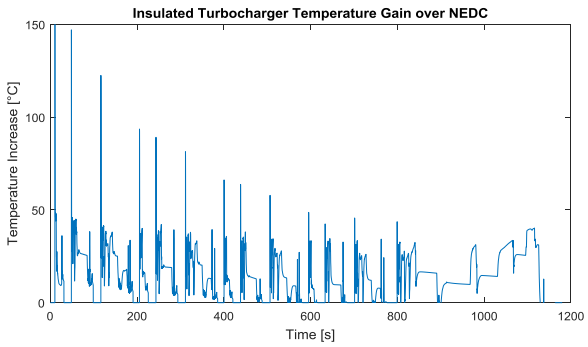

Figure 19: Difference in turbine outlet temperature over NEDC duty cycle between standard and inner-insulated turbochargers

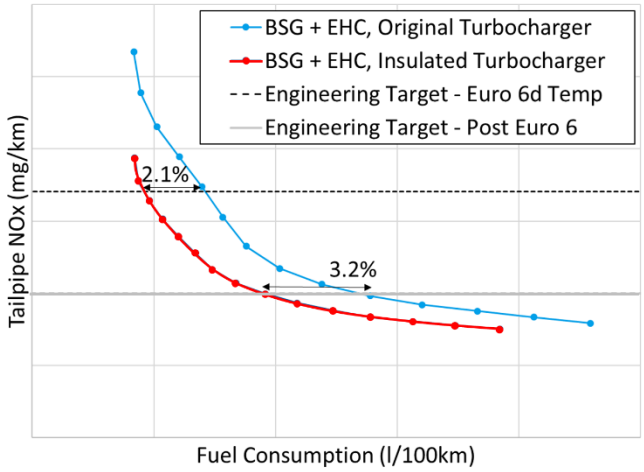

Figure 20: Difference in predicted Tailpipe NOx and fuel consumption between insulated and standard turbocharger in the RDE cycle

Little benefit was predicted for the insulated turbocharger over the WLTC duty cycle. However, there is greater benefit from the insulated turbocharger under low operating load conditions, where the lower exhaust temperatures lead to significant electric heating requirements. In order to evaluate this, the NEDC was simulated which represents a close to worst case RDE cycle for the Diesel application. figure 20 shows the tailpipe NOx and the fuel consumption for the baseline turbocharger and the inner-insulated turbocharger – with both vehicles utilising the BSG (Belt Starter Generator) and electrically heated catalyst (EHC). Applying an RDE engineering target for Euro 6d Temp (the legislation level used for the demonstrator vehicles), shows a 2.1% fuel consumption benefit from the inner-insulated turbocharger due to reduced energy usage from the EHC. Emissions legislation beyond Euro 6 is far from being finalised, but based available information at this time, the fuel consumption benefit of the inner-insulated turbocharger has the potential to reach 3.2%. While the NEDC represents a close to worst case RDE cycle, more challenging conditions apply in the real world, such as a congested city environment. Under these real-world conditions, it can be expected that the insulated turbocharger has the potential for even greater real-world fuel economy improvements than those presented over the NEDC below.

Conclusions

A thermally inner-insulated turbocharger is proposed for increasing T4 (to lower catalyst light-off time), which does not require any control modification and can be implemented easily. With the aerodynamic performance of the insulated and standard (non-insulated) turbochargers being almost identical, any change in T4 is entirely due to the inner-insulation. The objective of this work was to quantify the benefits of the inner-insulated turbocharger.

3D modelling was performed using uni-directional coupling of energy equation as with minor adjustments to the existing CAE models it enables them to compute full transient energy balances of the turbocharger. The 3D simulation was used to simulate a thermal-shock cycle which showed the inner-insulated turbocharger has reduced heat flux by 50-70% compared to the standard turbocharger. These results were used to parameterise a simple 1D lumped capacitance model which was capable of predicting similar aerodynamic behaviour of the two turbines. When compared with experimental results, the model was shown to over-estimate the benefits of the inner-insulation, although at this stage it is not known if this is caused by the model or the low load experimental conditions used.

The model was used within a system optimization tool to demonstrate the potential benefit in terms of fuel economy of the inner-insulated turbocharger when used in combination with an electrically heated catalyst. The largest benefits were predicted over the NEDC cycle which is representative of a low load real driving emissions cycle in cities. At iso-NOx emissions, the predicted benefits in fuel consumption were around 3%.

References

1. Hamedi, M.R., Doustdara, O., Tsolakisa, A., Hartlandb, J., *Thermal energy storage system for efficient diesel exhaust aftertreatment at low temperatures.* Applied energy, 2019. **235**: p. 874-887, https://doi.org/10.1016/j.apenergy.2018.11.008
2. (EU), C.I.R., *setting out a methodology for determining the correlation parameters necessary for reflecting the change in the regulatory test procedure with regard to light commercial vehicles and amending Implementing Regulation (EU).* 2017. **No. 293/2012**.
3. Ramanathan, K., D.H. West, and V. Balakotaiah, *Optimal design of catalytic converters for minimizing cold-start emissions.* Catalysis today, 2004. **98**(3): p. 357-373.
4. Korin, E., Reshef, R., Tshernichovesky, D., & Sher, E. (1999). Reducing cold-start emission from internal combustion engines by means of a catalytic converter embedded in a phase-change material. *Proceedings of the Institution of Mechanical Engineers, Part D: Journal of Automobile Engineering*, *213*(6), 575–583. https://doi.org/10.1243/0954407991527116
5. Luján, J.M., Bermúdez, V., Piqueras, P., García-Afonso, O., *Experimental assessment of pre-turbo aftertreatment configurations in a single stage turbocharged diesel engine. Part 1: Steady-state operation.* Energy, 2015. **80**: p. 599-613. https://doi.org/10.1016/j.energy.2014.05.048

6. Knoll, M., M. Kühn, and J. Boettcher, *Verbessertes Thermomanagement durch neue Isolationssysteme.* MTZ-Motortechnische Zeitschrift, 2018. **79**(2): p. 52-57.
7. Hu, B., *Application of divided exhaust period and variable drive supercharging concept for a downsized gasoline engine*. 2016, University of Bath UK.
8. Kunde, O., et al. *The new 2.0 SCTi EcoBoost gasoline engine from Ford*. in *19th Aachen Colloquium*. 2010.
9. Fricke F, Bhardwaj OP, Holderbaum B, Scofield T, Grußmann E, Kollmeier M. Investigation of Insulated Exhaust Manifolds and Turbine Housings in Modern Diesel Engines for Emissions and Fuel Consumption Reduction. SAE International; 2016. https://doi.org/10.4271/2016-01-1003
10. Marelli S, Usai V, Capobianco M, Montenegro G, Della Torre A, Onorati A. Direct Evaluation of Turbine Isentropic Efficiency in Turbochargers: CFD Assisted Design of an Innovative Measuring Technique. SAE International; 2019. https://doi.org/10.4271/2019-01-0324
11. Marelli S, Marmorato G, Capobianco M, Boulanger J-M. Towards the Direct Evaluation of Turbine Isentropic Efficiency in Turbocharger Testing. SAE International; 2016. https://doi.org/10.4271/2016-01-1033
12. Baar R, Biet C, Boxberger V, Zimmermann R. New Evaluation of Turbocharger Components based on Turbine Outlet Temperature Measurements in Adiabatic Conditions. IQPC-Tagung DOWNSIZING & TURBOCHARGING; 25/03/2014; Dusseldorf, Germany2014.
13. Cormerais M, Hetet JF, Chesse P, Maiboom A. Heat Transfer Analysis in a Turbocharger Compressor: Modeling and Experiments, SAE Paper Number 2006-01-0023. SAE International; 2006.
14. Özdemir, S., *Wärmestromanalyse der Radialturbinenstufe eines PKW-Abgasturboladers mittels numerischer Simulation.* 2017.
15. Serrano J, Olmeda P, Arnau F, Reyes-Belmonte M, Lefebvre A. Importance of Heat Transfer Phenomena in Small Turbochargers for Passenger Car Applications. SAE Int J Engines. 2013;6(2):716-28.
16. Bohn, D., T. Heuer, and K. Kusterer, *Conjugate flow and heat transfer investigation of a turbo charger.* Journal of engineering for gas turbines and power, 2005. **127**(3): p. 663-669.
17. Burke, R., Copeland, C.D., Duda, T. and Rayes-Belmote, M. A., *Lumped capacitance and three-dimensional computational fluid dynamics conjugate heat transfer modeling of an automotive turbocharger.* Journal of Engineering for Gas Turbines and Power, 2016. **138**(9): p. 092602.
18. Olmeda P, Dolz V, Arnau FJ, Reyes-Belmonte MA. Determination of heat flows inside turbochargers by means of a one dimensional lumped model. Mathematical and Computer Modelling. 2013;57(7-8):1847-52.
19. Serrano, J., García-Cuevas lng, L., Tiseira, A., Rodriguez Usaquen, T. et al., "Fast 2-D Heat Transfer Model for Computing Internal Temperatures in Automotive Turbochargers," SAE Technical Paper 2017-01-0513, 2017, https://doi.org/10.4271/2017-01-0513.
20. Baines, N., K.D. Wygant, and A. Dris, *The analysis of heat transfer in automotive turbochargers.* Journal of Engineering for Gas Turbines and Power, 2010. **132**(4): p. 042301.
21. Romagnoli, A. and R. Martinez-Botas, *Heat transfer analysis in a turbocharger turbine: An experimental and computational evaluation.* Applied Thermal Engineering, 2012. **38**: p. 58-77.
22. Romagnoli, A., Manivannan, A., Rajoo, S., Chiong, M.S., Feneley, A., Pesiridis, A., Martinez-Botas, R.F., *A review of heat transfer in turbochargers.* Renewable and Sustainable Energy Reviews, 2017. **79**: p. 1442-1460.
23. Serrano, J., Olmeda, P., Arnau, F., Dombrovsky, A. *General procedure for the determination of heat transfer properties in small automotive turbochargers.* SAE International Journal of Engines, 2015. **8**(1): p. 30-41.
24. Shaaban, S., *Experimental investigation and extended simulation of turbocharger non-adiabatic performance*. 2004, Verlag nicht ermittelbar.
25. Cormerais, M., P. Chesse, and J.-F. Hetet, *Turbocharger heat transfer modeling under steady and transient conditions.* International Journal of Thermodynamics, 2009. **12**(4): p. 193.
26. Burke RD, Vagg CRM, Chalet D, Chesse P., *Heat transfer in turbocharger turbines under steady, pulsating and transient conditions.* International Journal of Heat and Fluid Flow, 2015. **52**: p. 185-197.
27. Reyes Belmonte, M.A., *Contribution to the experimental characterization and 1-D modelling of turbochargers for IC engines*. 2014.
28. Vijayakumar, R., Burke, R.D., Liu, Y., Turner, J. W.G., *Design of an Advanced Air Path Test Stand for Steady and Transient Evaluation*. in *ASME 2018 Internal Combustion Engine Division Fall Technical Conference*. 2018. American Society of Mechanical Engineers.
29. Kroll, M. and B. Henrich, *Innenliegende Isolierung für ein mehrteiliges Turboladergehäuse.* MTZ-Motortechnische Zeitschrift, 2015. **76**(5): p. 42-47.
30. Zimmermann, R., B. Savic, and R. Baar. *Erweiterte Turboladermodellbildung Mittels Heißgasprüfstandsdaten, Eine Retrospektive Und Ausblickeines Innovativen Ansatzes*. in *Aufladetechnische Konferenz, Dresden, Germany*. 2017.
31. Marelli S, Gandolfi S, Capobianco M. Heat Transfer Effect on Performance Map of a Turbocharger Turbine for Automotive Application. SAE International; 2017. https://doi.org/10.4271/2017-01-1036
32. El-Sharkawy, A.E., *Analysis of Thermocouple Temperature Response under Actual Vehicle Test Conditions*. 2008, SAE Technical Paper.

Contact Information

Dr Richard Burke CEng, FIMechE
Department of Mechanical Engineering
University of Bath
Bath, BA2 7AY, UK
+44 01225 383481
R.D.Burke@bath.ac.uk

Acknowledgments

This work was conducted with funding from the THOMSON project which has received funding from the European Union's Horizon 2020 Programme for research, technological development and demonstration under Agreement no. 724037.

Nomenclature

A	Area of the surface	m^2
a	Coefficient in the Nusselt number equation	
b	Exponent for Reynolds number	
$c_{p\ Air}$	Specific heat at constant pressure of air	J/kgK
$c_{p\ Exh}$	Specific heat at constant pressure of exhaust gas	J/kgK
$\dot{m}_C$	Flow rate through the compressor	kg/s
$\dot{m}_T$	Mass flow rate through turbine	kg/s
$\dot{m}_{Tred}$	Reduced turbine mass flow rate	kg/s
Nu	Nusselt number	
Pr	Prandtl Number	
Q	Heat flow	W
Re	Reynolds number	
T	temperature	K
T_{1t}	Compressor total inlet temperature	K
T_{3t}	Total turbine inlet temperature	K

Greek Symbols

ε	Emissivity	
μ_bulk	Fluid viscosity at the bulk fluid temperature	N/m^2s
μ_skin	Fluid viscosity at the heat-transfer boundary surface temperature	N/m^2s
π_{comp}	Compressor pressure ratio	
π_{exp}	Turbine expansion ratio	
κ_{Air}	Specific heat ratio of air	
κ_{exh}	Specific heat ratio of exhaust gas	
$\eta_{is\ C}$	Isentropic Compressor efficiency	
$\eta_{is\ T}$	Turbine isentropic efficiency	
η_m	Mechanical efficiency of the turbocharger	
η_T	Turbine efficiency	
σ	Stefan-Boltzmann constant	W/m^2T^4

Definitions/Abbreviations

AFR	Air-Fuel Ratio
BSG	Belt Starter Generator
CAD	Computer Aided Design
CAE	Computer Aided Engineering
CFD	Computation Fluid Dynamics
CHT	Conjugate Heat Transfer
CO	Carbon monoxide
CO2	Carbon di oxide
DOC	Diesel Oxygen Catalyst
DPF	Diesel Particulate Filter
EAT	Exhaust gas aftertreatment
EGR	Exhaust Gas Recirculation
EHC	Electrically Heated Catalyst
FEA	Finite Element Analysis
FEM	Finite Element Modelling
HC	Hydro carbon
HT	Heat Transfer
HTC	Heat Transfer Coefficient
NEDC	New European Driving Cycle
NOx	Oxides of Nitrogen
RDE	Real Driving Emission
T/H	Turbine Housing
WLTC	Worldwide Harmonized Light Vehicles Test Cycle